J Arid Land (2025) 17(11): 1542–1557
doi: 10.1007/s40333-025-0033-7; CSTR: 32276.14.JAL.02500337

Science Press Springer-Verlag

Spatial trends of extreme temperature events and climate change indicators in climate zones of Jordan

Abdelaziz Q BASHABSHEH[1*], Kamel K ALZBOON[1], Zeyad ALSHBOUL[2]

[1] Department of Environmental Engineering, Al-Huson University College, Al-Balqa Applied University, Irbid 21510, Jordan;
[2] Faculty of Engineering, Department of Civil Engineering, Ajloun National University, Ajloun 26810, Jordan

Abstract: Extreme temperature events have intensified across Jordan over the past 40 a, increasing risks to agriculture, water availability, urban infrastructure, and public health. The purpose of this study is to assess the long-term spatial trends and regime shifts in extreme temperature indicators across Jordan's climate zones to explore climate adaptation strategies. This study presents a high-resolution and spatially explicit assessment of thermal extremes using daily data from 1982 to 2024 across 45 grid-based study points in Jordan. Thirteen temperature indices, including percentile-based thresholds, duration metrics, and absolute extremes, were computed using RClimDex and analyzed across four Köppen climate zones: hot desert (BWh), hot semi-arid (BSh), cold desert (BWk), and Mediterranean (Csa) climates. The analysis confirmed a statistically significant warming trend: annual mean maximum temperatures increased by 2.198°C, while annual mean minimum temperatures rose by 2.035°C. Cold extremes have sharply declined, with cold days (TX10p) decreasing by 70.0%–80.0%, and the cold spell duration indicator (CSDI) dropping from 12.6 to 4.0 d/a, particularly in the BWk zone. Heat indices intensified across all zones, with warm days (TX90p) increasing by over 300.0% in BWh, warm nights (TN90p) rising by 38.1%, and the warm spell duration indicator (WSDI) extending fourfold, indicating prolonged exposure to heatwaves. Mean value of maximum temperature (TXx) reached 45.600°C in most arid areas, while minimum temperature (TNx) exceeded 31.600°C, highlighting increased nocturnal heat stress. Change-point analysis indicated that 1998 was a pivotal year, marking a structural transition in both cold and warm temperature indices. Subsequent intensifications after 2010 in TN90p, TNx, and mean of daily maximum temperature ($T_{maxmean}$) reflected an ongoing trend toward sustained thermal extremes. In addition to time-series trends, the study employed network-based correlation analysis to explore the coherence among climate indices. Strong positive correlations were observed among TXx, TX90p, and mean of daily minimum temperature ($T_{minmean}$) ($r \geq 0.94$), as well as among TN90p, $T_{minmean}$, and TNx ($r \geq 0.87$), indicating a tightly clustered heat subsystem. Duration metrics like the WSDI showed a close alignment with percentile extremes (between WSDI and TX90p; $r = 0.88$), suggesting integrated heatwave behavior. In contrast, cold indices (TX10p, TN90p, frost days, and CSDI) exhibited weak or negative correlations and displayed peripheral positioning in the climate network, indicating their limited role under a warming regime. Absolute extremes showed weak internal linkages, suggesting episodic rather than systemic response characteristics. This structural realignment indicated a shift from a previously balanced thermal profile to a heat-dominated climate system. Regional variations revealed that BWh and BSh were experiencing the steepest warming, while Csa was transitioning more slowly but was showing signs of reduced winter cooling and increased irrigation demands. The findings establish a robust climate baseline for Jordan and offer actionable insights for climate adaptation planning. Recommended measures include precision irrigation, the development of heat-resilient crops, improvements to urban cooling infrastructure, and early warning systems for thermal extremes. By integrating spatial climate zoning, regime shift analysis, and inter-index correlation structures, this study provides a replicable framework for monitoring climatic transformations and informing resilience strategies in arid and semi-arid areas.

*Corresponding author: Abdelaziz Q BASHABSHEH (E-mail: abdelazizbashabsheh@gmail.com)
Received 2025-06-03; revised 2025-08-30; accepted 2025-10-05

Keywords: climate change; extreme events; arid area; temperature trends; weather shift; Köppen climate classification; Jordan

Citation: Abdelaziz Q BASHABSHEH, Kamel K ALZBOON, Zeyad ALSHBOUL. 2025. Spatial trends of extreme temperature events and climate change indicators in climate zones of Jordan. Journal of Arid Land, 17(11): 1542–1557. https://doi.org/10.1007/s40333-024-0033-7; https://cstr.cn/32276.14.JAL.02500337

1 Introduction

Climate change is accelerating globally due to the ongoing rise in greenhouse gas (GHG) concentrations especially carbon dioxide, methane, and nitrous oxide that come from the combustion of fossil fuels, industrial activities, and changes in land use (IPCC, 2022). These elevated GHG levels have triggered widespread transformations in the Earth's climate system, leading to rising global temperatures, altered precipitation patterns, and increasing occurrences of extreme weather events, such as heatwaves, floods, droughts, and tropical cyclones (Cheng et al., 2021; IPCC, 2023). The global mean surface temperature rose by approximately 1.100°C–1.200°C above pre-industrial levels between 2011 and 2020, with 2023 showing around a 1.450°C increase (WMO, 2024). These warming trends have resulted in glacial retreat, rising sea levels, marine heatwaves, coral bleaching, and disruptions to ecosystems (IPCC, 2019; WMO, 2024). In low-income areas, these impacts have exacerbated inequalities and threatened food and water security, health systems, and economic stability (UNEP, 2022). Without immediate mitigation efforts, warming may exceed 2.000°C–4.000°C by 2100, leading to even more frequent and severe climate events (IPCC, 2023).

Extreme climate events are particularly vulnerable to climate change, often causing substantial damage in short periods, ranging from days to weeks (Cheong et al., 2018; Perera et al., 2020). Between 2000 and 2019, over 11×10^3 extreme climate events resulted in the deaths of more than 475×10^3 people and incurred economic losses of around 2.56×10^{12} USD across both public and private sectors (Eckstein et al., 2021). On a continental level, Europe has faced numerous extreme climate events, particularly heatwaves. France experienced severe heatwaves in 2003, 2006, 2015, and 2022, resulting in approximately 27×10^3 deaths. Similarly, the Russian Federation recorded 55×10^3 deaths in heatwave of 2010 (Hoag, 2014; Douris and Kim, 2021; Pascal et al., 2024). Floods and storms have also led to significant economic losses, with Germany and Italy suffering damages of 37×10^9 and 28×10^9 USD, respectively. In Africa, water-related disasters tied to extreme events have accounted for 35.0% of climate-related deaths and 1.0% of global economic losses over the past fifty years (Douris and Kim, 2021).

Jordan, one of the world's most water-scarce countries, is particularly vulnerable to these changes. Recent analyses indicate marked increases in temperature extremes and declining precipitation, which have significant implications for water availability, public health, and infrastructure resilience. Smadi (2006) identified abrupt changes and a significant warming trend of 0.038°C/a at the airport station in Amman, while it has been recorded an increase in mean maximum and minimum temperatures of 1.620°C and 1.390°C, respectively, in northern Yarmouk Basin of Jordan, contributing to reduced streamflow due to intensified evapotranspiration (Bashabsheh and Alzboon, 2024). At the national scale, the CoKriging technique has been applied to analyze climate variability using elevation data, revealing a rise in temperature and evapotranspiration alongside a decline in precipitation of 1.2 mm/a (Al-Qinna, 2018). Similarly, Alzboon et al. (2021) used the area method to trace temperature trends across ten stations, highlighting shifts in seasonal temperature thresholds, including a delayed onset of cold months and an expansion of extreme heat periods.

Human vulnerability to climate extremes is increasing. Alwadi et al. (2024) quantified mortality burdens in Amman, showing that non-Jordanians face a greater risk of cold-related health issues, while females are more sensitive to heat. A companion study by Alwadi et al. (2024) found an average of 6.5 heat-attributable deaths per day in Amman beyond critical thresholds, emphasizing the urgent need for heat action planning. Heatwaves, in particular, show rapid

intensification. Broader analyses further confirmed long-term increases in minimum temperatures and diminishing diurnal temperature ranges and signs of enhanced radiative trapping in the atmosphere (Hamdi et al., 2009; Abu-Allaban et al., 2015). Although Jordan boasts a diverse ecology, ranging from arid deserts to Mediterranean highlands, there have been few comprehensive spatial assessments of climate across the country. Projections of Jordan's future climate indicate a worrying trend of increased extreme weather events. Recent high-resolution modeling for the Yarmouk Basin forecasts a future with significantly more heatwaves, prolonged droughts, and more volatile hydro-climatic conditions (Bashabsheh and Alzboon, 2025). These projections underscore the urgency of establishing a robust climate baseline and spatially explicit analysis of temperature extreme. This research seeks to fill that gap by utilizing high-quality temperature data from 45 weather stations and employing internationally recognized indices through the RClimDex platform (Zhang and Yang, 2004). The study applies the Köppen climate classification to examine regional disparities in climate extremes, which is essential for informing local adaptation efforts (Köppen and Wegener, 2015).

This study showed its integration of percentile and duration-based temperature indices with spatial climate zoning, which reveals structural shifts in Jordan's thermal regime. Additionally, this study includes correlation-based network analysis, providing a unique perspective on the relationships among climate indicators. This analysis also highlights clustering behavior and underscores the decreasing significance of cold extremes, an aspect that is seldom explored in regional studies. Moreover, this study establishes a solid baseline for monitoring risks and planning for climate resilience by connecting long-term temperature trends to local vulnerabilities and incorporating spatial climate variability. Finally, it might offer methodological innovations that can be applied to other arid and semi-arid areas.

2 Materials and methods

Jordan is a country that locates in the southwest of Asia and shares borders with Syria to the north, Palestine to the west, Saudi Arabia to the south, and Iraq to the east (29°11′–33°38′N, 35°25′–39°18′E; Fig. 1). The terrain of Jordan is divided into three types namely: the Jordan valley, the mountainous highlands, and the desert plateau (Al-Bilbisi, 2013). Climate varies from Mediterranean in the west to desert in the east and south. Summers are characterized by high temperatures and low humidity, making even temperatures in the low 30.000°C feel relatively bearable (Hazaymeh et al., 2024). Summer temperatures in Jordan rarely exceed 35.000°C. Winters are wetter and relatively cold, especially in the highlands, while autumn serves as a transitional period with gradually cooling temperatures and minimal precipitation (Atashi et al., 2020). The study area was divided by climatic zones, as temperature patterns are closely associated with these zones. This classification facilitated the analysis of how extreme climate events vary across different areas. According to the Köppen climate classification system (Köppen and Wegener, 2015), we categorized Jordan into four climatic zones: Mediterranean climate (Csa), hot semi-arid climate (BSh), cold desert climate (BWk), and hot desert climate (BWh) (World Bank Group, 2025).

Extreme events in Jordan have been analyzed over the past four decades by use of accurate and long-term daily temperature data that comprehensively covers all study areas without gaps or missing years. Data of daily temperatures were obtained from power data access viewer of the National Aeronautics and Space Administration (NASA) (https://power.larc.nasa.gov/data-access-viewer/). Many studies examined the reliability of datasets obtained from NASA for different climatic zones by comparing the obtained data and measured temperature data. The data have demonstrated its reliability in hot desert and Mediterranean climates as well as additional international assessments from South Asia and Xizang Plateau in China further support its broader applicability (Zhu et al., 2019; Ali et al., 2021; Baig et al., 2021; Marzouk, 2021; Rodrigues and Braga, 2021; Hussain et al., 2022).

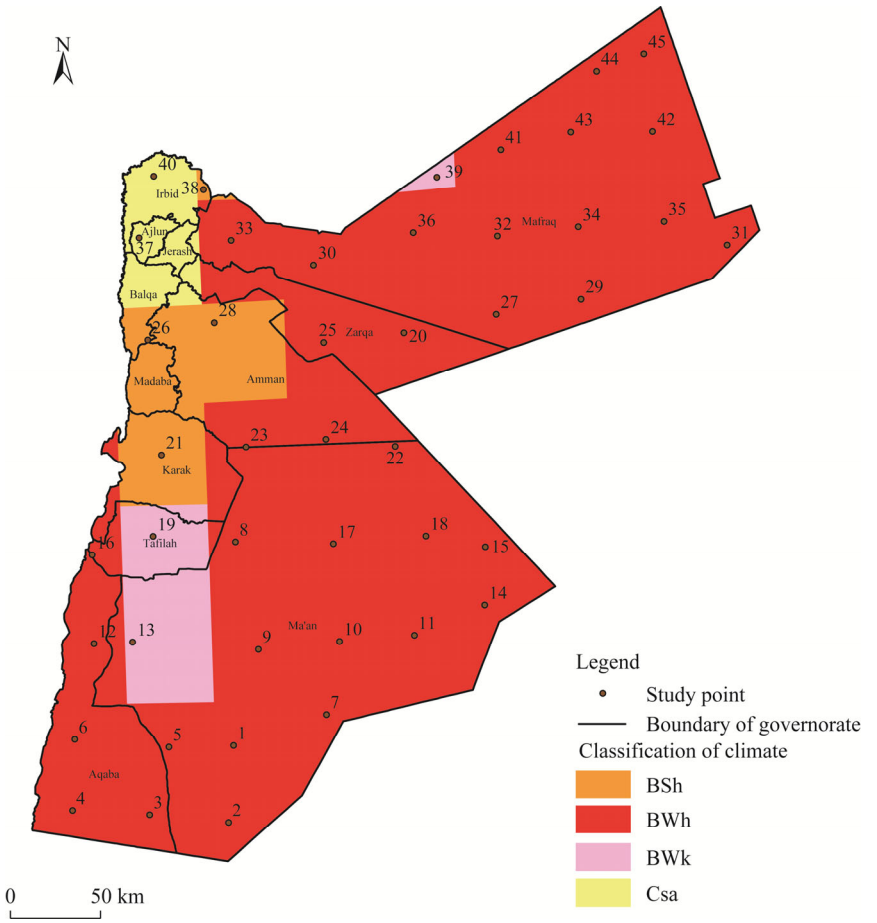

Fig. 1 Map of the study area showing Jordan's governorates, numbered study points, and climate zones classified according to the Köppen climate classification. BSh, hot semi-arid climate; BWh, hot desert climate; BWk, cold desert climate; Csa, Mediterranean climate.

Daily minimum and maximum temperatures were obtained from 45 grids to cover all of Jordan from 1982 to 2024, as shown in Figure 1. The Climatol package in R v.3.6.1 software was utilized for quality control, homogenization, and statistical analysis of temperature data for ensuring consistency and reliability (Guijarro, 2018). To assess changes in temperature extremes, this study employed RClimDex, an R-based software developed by Environment Canada, which calculates 27 internationally recognized climate indices (Zhang and Yang, 2004; Zhang et al., 2011). Although the full suite includes 16 temperature and 11 precipitation indices, this research specifically selected 13 temperature-based indices that are most relevant to extreme heat and cold events affecting Jordan's climatic zones, which shown in Table 1. Least-squares regression method was applied for assessing trends of variables by use of RClimDex package. Student's *t*-test was performed to test the null hypothesis and trends were considered at significant level of 0.05 (Easterling et al., 2003). To identify statistically significant regime transitions in extreme temperature indices, we applied Change-Point Analyzer (CPA), a robust non-parametric tool developed by Taylor Enterprises (https://variation.com/product/change-point-analyzer/).

3 Results

3.1 Time series analysis of temperature extremes

3.1.1 Cold extremes and frost days reduction

Figure 2 shows the changes of temperature extremes. TX10p, representing the percentage of days

Table 1 Temperature indices and definitions

No.	Abbreviation	Indicator name	Definition	Unit
1	FD0	Frost days	Days when daily minimum temperature (TN)<0.000°C	d
2	TXx	Maximum T_{max}	Monthly maximum value of daily maximum temperature (TX)	°C
3	TNx	Maximum T_{min}	Monthly maximum value of TN	°C
4	TXn	Minimum T_{max}	Monthly minimum value of TX	°C
5	TNn	Minimum T_{min}	Monthly minimum value of TN	°C
6	TN10p	Cold nights	Percentage of days when TN<10^{th} percentile	%
7	TX10p	Cold days	Percentage of days when TX<10^{th} percentile	%
8	TN90p	Warm nights	Percentage of days when TN>90^{th} percentile	%
9	TX90p	Warm days	Percentage of days when TX>90^{th} percentile	%
10	WSDI	Warm spell duration indicator	Days with at least 6 consecutive days when TX>90^{th} percentile	d
11	CSDI	Cold spell duration indicator	Days with at least 6 consecutive days when TN<10^{th} percentile	d
12	$T_{maxmean}$	Mean of daily maximum temperature	Annual mean of TX	°C
13	$T_{minmean}$	Mean of daily minimum temperature	Annual mean of TN	°C

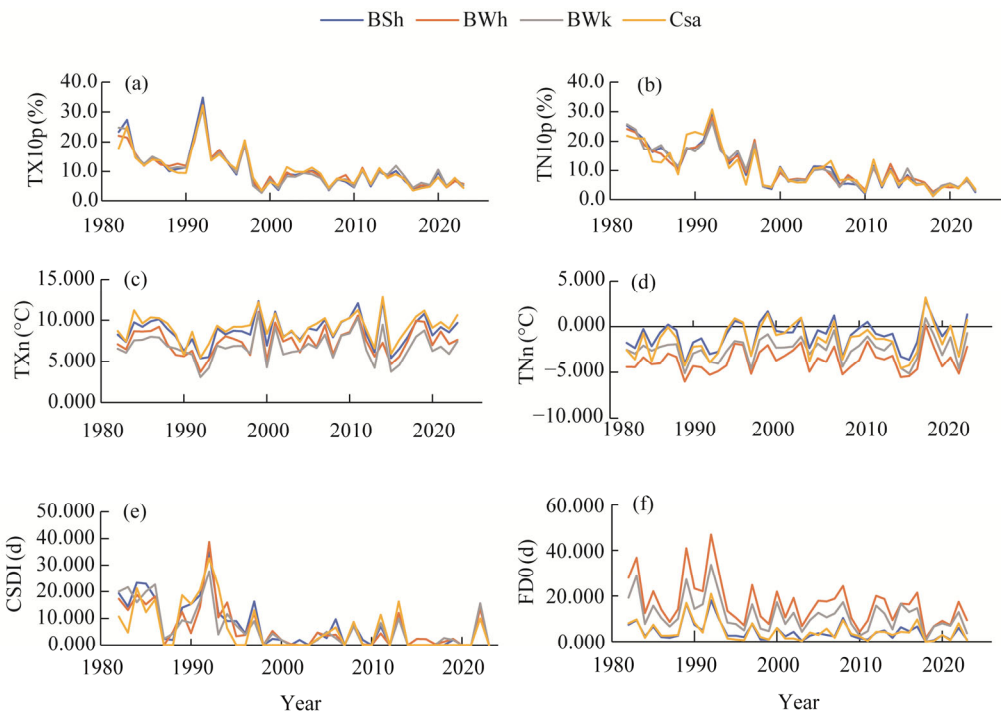

Fig. 2 Average trends for cold indices for the BSh (hot semi-arid), BWh (cold desert), BWk (hot desert), and Csa (Mediterranean) zones from 1982 to 2024. (a), TX10p (percentage of days when daily minimum temperature (TN)<10^{th} percentile); (b), TN10p (percentage of days when daily maximum temperature (TX)<10^{th} percentile); (c), TXn (monthly minimum values of daily maximum temperature); (d), TNn (monthly minimum values of daily minimum temperature); (e), CSDI (cold spell duration indicator); (f), FD0 (days when TN<0.000ºC).

with maximum temperatures below the 10^{th} percentile, showed a significant decline in cold daytime extremes across all of Jordan from 1982 to 2024 (Fig. 2a). The sharpest drops occurred in 1999 and 2007, with values falling to 2.7%–4.5%, notably below the 10.0% threshold. In contrast, the weather in 1992 was exceptionally cold in the BWh zone, reaching up to 34.8%. Similarly, TN10p, measuring nights with minimum temperatures below the 10^{th} percentile, also decreased

steadily (Fig. 2b), with values ranging from 18.0% to 34.0% in 1992 and later dropping to 2.0%–3.0%.

The CSDI also highlighted a downward trend (Fig. 2e), especially in the BSh and BWh zones, where cold spells reduced to 2.400 d in 1999 and 4.200 d in 2007. Meanwhile, the intensity indices TXn and TNn increased over time (Fig. 2c and 2d), signaling milder cold extremes. TXn reached 11.400°C in 1999 and 13.200°C in 2007, compared with the lowest value 6.800°C in 1992.

The FD0 index indicated a decline across all zones (Fig. 2f), particularly in the BWh zone, with values dropping below 5.000 d annually by the late 1990s. Trend analysis confirmed significant reductions in cold extremes, with average annual slope decline for TX10p and TN10p across zones ranging from –0.312°C/a to –0.447°C/a, respectively. Over the study period of approximately four decades, the TXn increased most in the Csa zone by 1.066°C, while the TNn rose even more (1.250°C), especially in the Csa zone.

3.1.2 Hot extremes and intense heatwaves

The TX90p index showed an increase in hot days across all climatic zones (Fig. 3a), peaking at 32.6%–36.4% in 1998, 2010, 2017, and 2021, particularly in the BWh and BSh zones. In contrast, the index showed milder values (10.0%–12.0%) in 1982 and 1992. The TN90p index also rose significantly (Fig. 3b), reaching 29.6%–33.5% in recent years, especially in desert zones. The TXx and TNx indices continued to rise (Fig. 3c and 3d), with TXx hitting 44.200°C–45.600°C and TNx reaching 29.400°C–31.600°C in the BWh and BSh zones during the peak years.

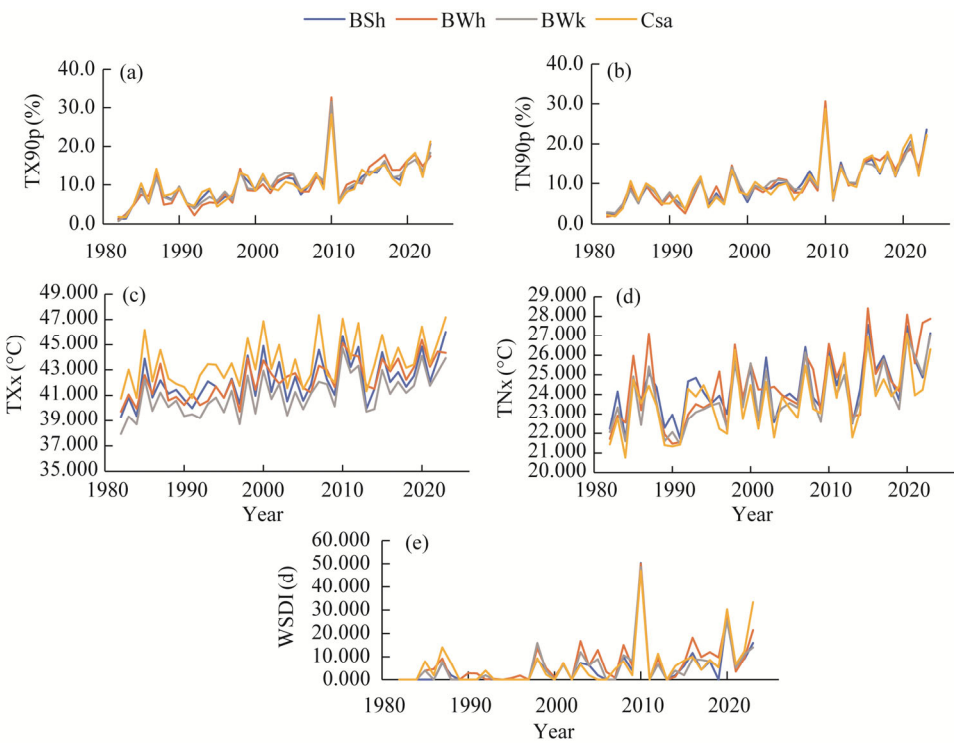

Fig. 3 Average trends for hot indices for the BSh, BWh, BWk, and Csa zones from 1982 to 2024. (a), TX90p (percentage of days when daily maximum temperature (TX)>90th percentile); (b), TN90p (percentage of days when daily minimum temperature (TN)>90th percentile); (c), TXx (monthly maximum value of TX); (d), TNx (monthly maximum value of TN); (e), WSDI (warm spell duration indicator).

The WSDI indicated longer heatwaves, with notable peaks in 1998, 2010, 2017, and 2021 extending to 13.200 d in the BSh zone and 15.800 d in the BWh zone (Fig. 3e). Conversely, shorter durations were recorded in 1982 (2.300 d) and 1992 (3.700 d). The WSDI trends showed a

pronounced slope increase in the BWh zone (0.523 d/a), followed by the BSh zone (0.487 d/a) and the BWk zone (0.412 d/a). Regarding temperature intensity, TXx increased by 1.430°C in the BWh zone and 1.188°C in the BSh zone, while TNx rose by 1.370°C in the BWh zone and 1.124°C in the BSh zone.

3.1.3 Long-term warming trend and shift of extreme cold to heat events

The $T_{maxmean}$ index showed a clear warming trend (Fig. 4a). The hottest years, 2010 and 2023, had $T_{maxmean}$ values of 29.400°C and 31.200°C, while the coldest years, 1982 and 1992, had $T_{maxmean}$ values of 24.100°C and 26.700°C, respectively. The BWh zone consistently had the highest values and steepest increase, while the Csa zone had a slower rise. Similarly, the $T_{minmean}$ index also displayed an upward trend (Fig. 4b), with the warmest years recording values of 14.700°C and 16.200°C in 2023 and 2010, compared with the values of 10.300°C–12.100°C in the coolest years. The BWh zone experienced the most considerable nighttime warming. Trend analysis showed that $T_{maxmean}$ slopes rose by 0.050°C/a–0.056°C/a in the BSh zone and 0.050°C/a–0.054°C/a in the BWk zone. At the national scale, averages increased by 2.198°C for $T_{maxmean}$ and 2.035°C for $T_{minmean}$ during the 40-a study period. This result indicated a pronounced warming signal across Jordan, with desert zones experiencing the strongest rise, while the Mediterranean zone exhibited comparatively slower warming.

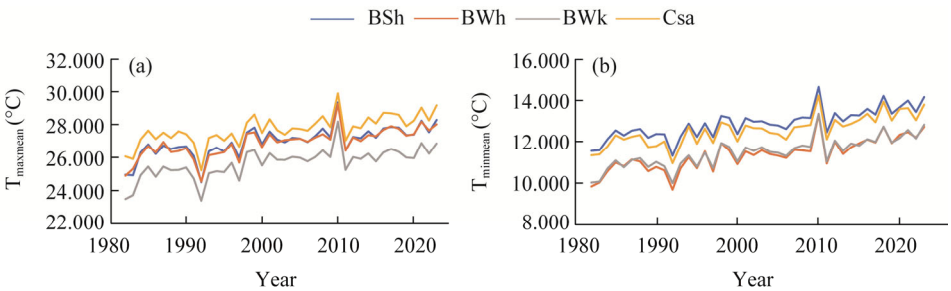

Fig. 4 Average trends of maximum and minimum temperatures for the BSh, BWh, BWk, and Csa zones from 1982 to 2024. (a), $T_{maxmean}$ (mean of daily maximum temperature); (b), $T_{minmean}$ (mean of daily minimum temperature).

3.2 Change-point analysis of temperature extremes

The change-point analysis confirmed statistically significant regime shifts across multiple temperature-based extreme indices, which aligned with visual inspections and ecological observations of the climatic transition in Jordan. Most of these shifts clustered around 1998, indicating a coordinated change affecting both cold and warm extremes. TX10p experienced a dramatic decline from 32.6% to 9.0% in 1993, followed by a further reduction of 5.8% in 2017. A significant decrease in its standard deviation was observed in 1998, suggesting not only fewer cold days but also reduced variability. CSDI exhibited a regime shift in 1995, with values dropping from 14.540 to 2.920 d/a. This reduction was visually confirmed in 1998, as the values fell to nearly zero across various zones. While TXn did not show a significant mean shift, its variability increased in 1998, with the standard deviation rising from 0.690°C to 1.680°C, indicating a wider range of extreme cold temperatures. FD0 index experienced two regime shifts: an initial increase from 10.790 to 19.670 d/a in 1989, followed by a sharp and sustained decline to 7.310 d/a in 1994, supporting the observed reduction in frost events. TN10p also displayed a coordinated decrease around 1998, falling from 17.7% to 6.5%, with no change in variability. Conversely, TNn did not reveal any statistically significant regime shifts or changes in variability, indicating stability in annual absolute minimum temperatures (Figs. 2–4).

TX90p index shifted in 1998 from 6.2% to 11.5%, with a subsequent increase to 15.0% in 2015, both transitions supported by 100.0% confidence and showing no significant change in variability. WSDI sharply increased in 1998 from 1.700 to 8.800 d/a, preceded by a subtler shift in 1985,

although the change in 1998 remained structurally dominant. TN90p exhibited two statistically significant transitions: an initial rise from 6.2% to 10.8% in 1998 followed by a further increase to 16.5% in 2015 (99.0% confidence), indicating stepwise nocturnal heat intensification. TXx rose from 41.200°C to 43.000°C in 1998, with no significant change in variability, suggesting a stable increase in extreme heat thresholds. TNx experienced a later regime shift in 2015, with annual TNx rising from 23.700°C to 25.680°C, reinforcing the trend of nocturnal warming after 2010. $T_{maxmean}$ increased from 25.990°C to 27.310°C in 1998, while $T_{minmean}$ followed a stepwise pattern, rising from 11.440°C to 12.190°C in 1998 then to 12.820°C in 2010, both without changes in variability, reinforcing consistent baseline warming trends (Figs. 2–4).

3.3 Frequency analysis of temperature extremes

From 1982 to 2024, Jordan's climatic zones showed a significant warming trend, with a significant decline in cold events and a rise in warm occurrences (Fig. 5). In the BWk zone, the percentage of cold days dropped from 19.7% (1982–1992) to 5.1% (2015–2024), while the BSh zone reduced from 16.8% to 3.4% (Fig. 5a). Percentage of cold nights also decreased, indicating fewer cold nighttime extremes (Fig. 5b). CSDI diminished from 12.600 d/a in the BWk zone to 4.000 d/a, and from 10.700 to 3.100 d/a in the BSh zone (Fig. 5c). Conversely, warm temperature extremes have surged, especially in desert zones. Percentage of hot days quadrupled overall, with the BWh zone increasing from 11.1% to 35.2% (Fig. 5e). Similarly, percentage of hot nights rose from 12.8% to 38.1% in the BWh zone, illustrating heightened nighttime heat retention (Fig. 5f). WSDI also extended significantly, from 5.400 d/a to 18.300 d/a in the BWh zone and 3.800 to 15.200 d/a in the BSh zone (Fig. 5g).

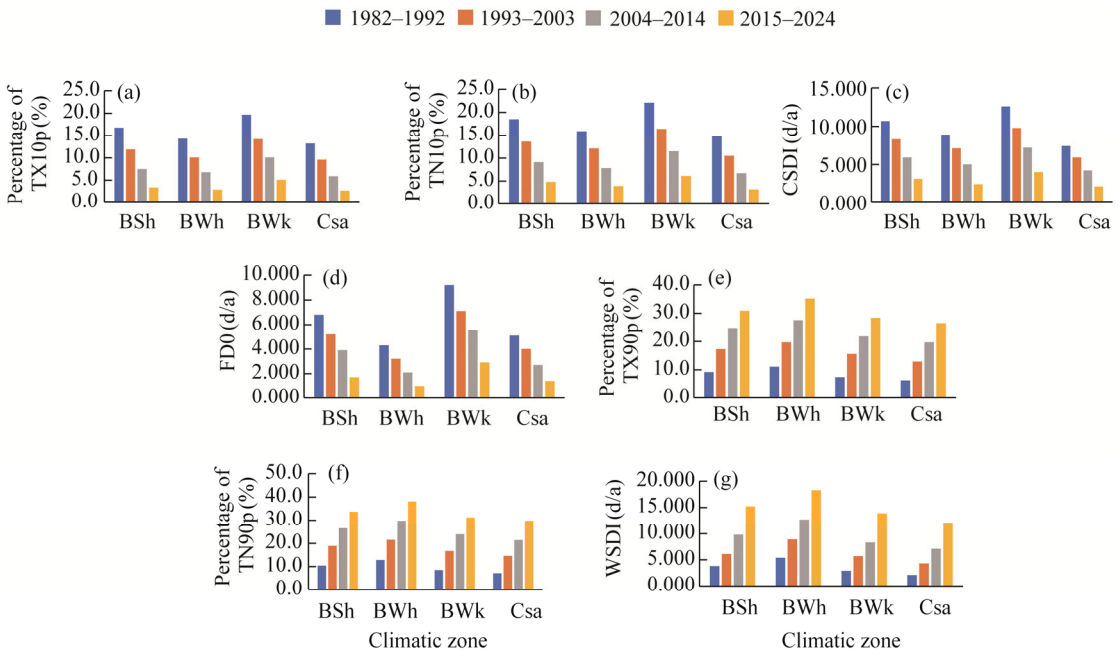

Fig. 5 Frequency distribution of extreme temperature events across climatic zones in Jordan from 1982 to 2024. (a), percentage of TX10p; (b), percentage of TN10p; (c), CSDI; (d), FD0, (e), percentage of TX90p; (f), percentage of TN90p; (g), WSDI.

A comparison of climatic zones confirmed the strongest warming trends in desert zones (BWh and BWk), with hot semi-arid zone (BSh) also showing significant increases, while the Mediterranean zone (Csa) exhibited a more gradual but statistically significant trend. Analysis of extreme temperatures revealed a distinct upward shift. The distribution of TXx showed a marked movement toward more extreme values, with the BWh zone displaying the most pronounced

intensification (Fig. 6a). Specifically, the BWh zone recorded the 40.000°C–42.000°C range within 18 a, reinforcing greater heat accumulation in deserts. Conversely, TXn zone revealed a steady decline in extreme cold occurrences (Fig. 6b), with frequencies within the 10.000°C–12.000°C range dropping significantly, particularly in desert zones.

Nocturnal warming was also severe. The TNx increased significantly, with the most extreme range (27.000°C–30.000°C) occurring for 12 a in the BWh zone (Fig. 6c). Concurrently, the TNn showed a diminishing presence of cold events: nights below 8.000°C were now rare, and the TNn had shifted to the 8.000°C–10.000°C range in the BWh zone (Fig. 6d), indicating reduced frost frequency. This pattern of sustained warming was further confirmed by mean temperatures. $T_{maxmean}$ showed higher intervals persisting for longer durations, with the 26.000°C–28.000°C range dominating the BWh zone for 16 a (Fig. 6e). Similarly, $T_{minmean}$ reinforced nighttime warming, with the 12.000°C–14.000°C range dominant in the BWh zone for 18 a (Fig. 6f), confirming a steady rise in minimum temperatures across all zones. This comprehensive analysis confirmed that desert regions experienced prolonged exposure to extreme heat, while all zones showed a consistent decline in cold events (Fig. 6a–f), signaling a fundamental shift in Jordan's climate dynamics and emphasizing the need for tailored climate adaptation strategies.

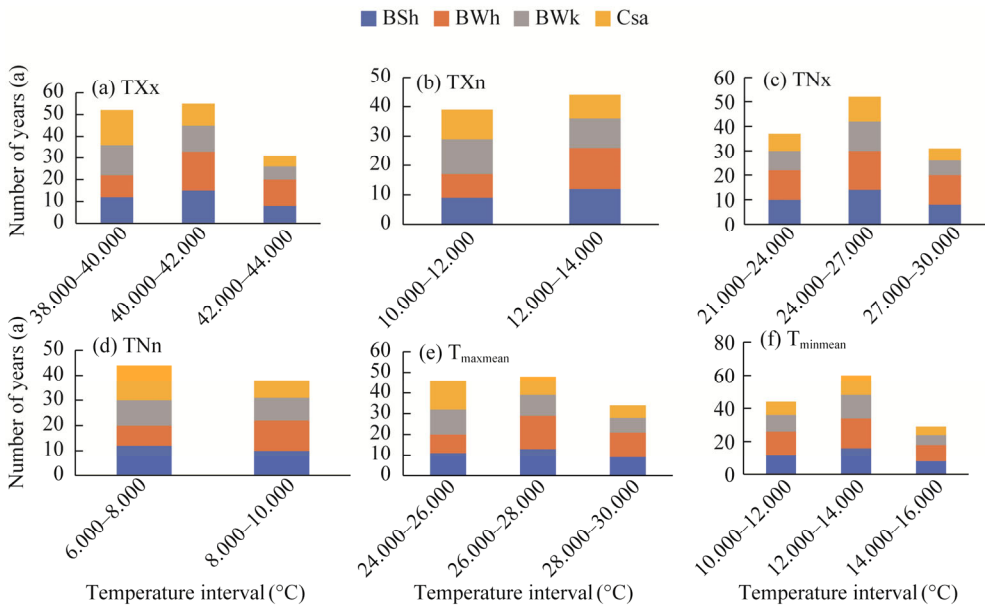

Fig. 6 Frequency distribution of temperature indices across climatic zones in Jordan from 1982 to 2024. (a), TXx; (b), TXn; (c), TNx; (d), TNn; (e), $T_{maxmean}$; (f), $T_{minmean}$.

3.4 Correlation between climate indices

Analysis of the Pearson's correlation matrix revealed a strong internal coherence among temperature-based climate indices (Fig. 7). This result highlights distinct behavioral clusters between warm and cold extremes. High positive correlations were found between TXx and TX90p (r=0.94), as well as between TXx and $T_{maxmean}$ (r=0.90). These correlations reflect the structural interdependence among extreme heat thresholds, hot-day frequency, and mean maximum temperatures. Similarly, TN90p and $T_{minmean}$ exhibited a strong association (r=0.87), indicating that increases in nocturnal heat events were concurrent with rises in baseline nighttime temperatures.

Duration-based indicators, such as WSDI, have also shown a close correlation with TX90p (r=0.82), emphasizing the link between prolonged heat spells and daytime heat intensity. In contrast, strong negative correlations were observed between TX10p and TXx (r= –0.85) and between TN10p and TN90p (r= –0.81). These findings support the idea of a coordinated thermal

shift, where cold extremes decrease as heat indicators intensify. Additionally, FD0 index displayed a notable inverse relationship with TX90p (r= –0.79), signifying a significant reduction in frost days accompanying warming trends. Meanwhile, indices representing absolute extremes, such as TXn and TNn, showed weak or negligible correlations with duration metrics, suggesting differentiated drivers or delayed responses. Collectively, these results validate the selection of indices and underscore a clustered network of warm indicators, reinforcing the emergence of a heat-dominated climate regime across Jordan.

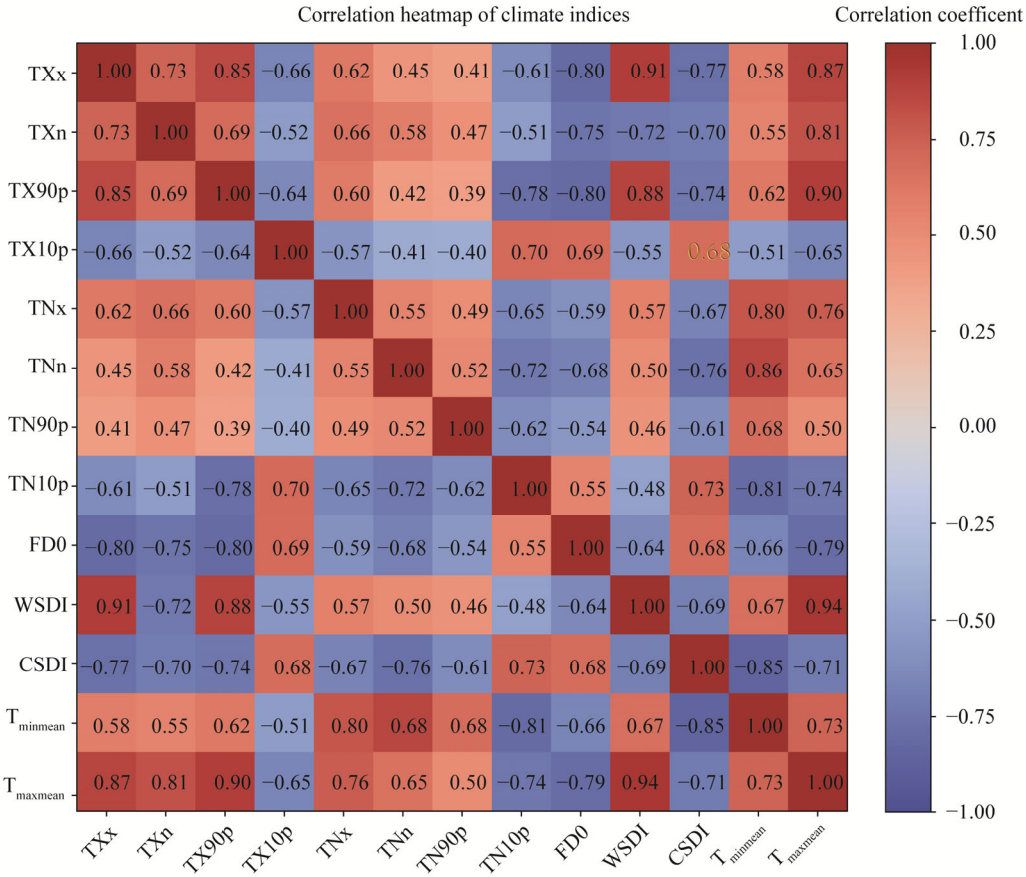

Fig. 7 Pearson's correlation of 13 climate indices used to evaluate thermal behavior and regime shifts

4 Discussion

4.1 Interpretation of warming trends and extreme events

The analysis indicates that Jordan is not just warming, and it is undergoing a fundamental shift from a climate characterized by seasonal variability to one dominated by persistent heat. Modeling conducted under the Representative Concentration Pathway 8.5 (RCP8.5) scenario suggests that heat waves could increase by as much as 22.000 d by the end of the century (Bashabsheh and Alzboon, 2025). Additionally, consecutive dry days may extend by over 65.000 d, further worsening drought stress. This result underscores the urgency of the trends outlined in this study. The most significant warming is occurring in desert zones (BWh and BWk), where maximum temperatures have risen by over 2.198°C. This trend is not isolated but serves as a key indicator of accelerated aridification. Meanwhile, this trend aligns with a global pattern where feedback loops, such as reduced soil moisture and vegetation cover, amplifying warming in drylands (Zhang et al., 2011; Linnenluecke et al., 2013; Safriel, 2017). The simultaneous

intensification of all heat extremes (TX90p, TN90p, and WSDI) and the decline of all cold extremes (TX10p, TN10p, and FD0) confirm that this transformation is systemic, rather than a change in isolated metrics. Identifying 1998 as a pivotal change point is crucial, as it suggests that Jordan's climate crossed a threshold into a new, more volatile state during a period of strong global forcing. The subsequent intensification after 2010 indicates that this new state continues to evolve toward greater extremity. Regional studies reinforce this trend, showing similar warming patterns and reductions in seasonal variability across Jordan and eastern Mediterranean (Alzboon et al., 2021; Zittis et al., 2022; Alsalal et al., 2024). This study adds methodological depth by integrating percentile-based indices, duration metrics, and network correlation structures, offering a spatially explicit and temporally robust assessment. Compared with earlier station-based studies (Bashabsheh and Alzboon, 2024, 2025), the use of RClimDex and change-point analysis provides stronger statistical validation and reveals coordinated shifts in climate behavior.

Correlation network analysis further supports this interpretation (Fig. 8). The strong clustering of heat indices indicates that they are now part of a tightly coupled and self-reinforcing system. In contrast, the peripheral and weakening position of cold indices suggests that they are becoming transient outliers in this new thermal regime. This structural realignment is consistent with tipping point behavior observed in other areas, indicating that a fundamental and likely irreversible reorganization of climate dynamics moves beyond a linear trend (Cheng et al., 2021; Armstrong McKay et al., 2022).

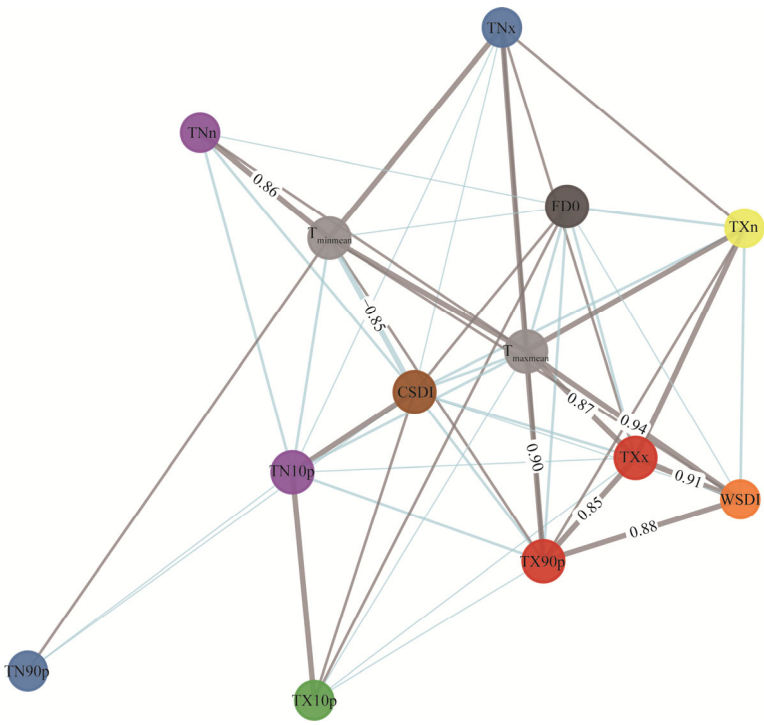

Fig. 8 Correlation-based climate index network illustrating statistically significant relationships among 13 climate indices

4.2 Sectoral impacts and vulnerabilities

The implications of increased heat extremes are significant for agriculture, water resources, and public health. In agriculture, elevated TX90p values and prolonged WSDI periods shorten crop growth cycles, reduce yields, and increase irrigation demands (Bisht et al., 2023; FAO, 2023). Warmer nighttime temperatures (TN90p and TNx) hinder plant recovery and increase transpiration, exacerbating drought stress. Crops that require chilling hours, such as olives and

grapes, are particularly vulnerable in the Csa and BWk zones (Zeppel et al., 2014).

Livestock, especially dairy cattle, suffer from heat-related metabolic disruptions, leading to reduced productivity (Cartwright et al., 2023). These agricultural challenges are worsened by Jordan's extreme water occurrence. Jordan ranks among the top five countries facing extreme water stress (Resource Watch, 2025), with groundwater extraction rates exceeding recharge rates and rising temperatures increasing evaporative losses (MoEnv, 2022). In the Yarmouk Basin, warming has led to decreased streamflow and increased rate of evapotranspiration (Bashabsheh and Alzboon, 2024). Climate data observed from 2006 to 2017 already exceeded projections from the high-emissions scenario RCP8.5, indicating a faster acceleration of warming and drought trends than previously modeled (Bashabsheh and Alzboon, 2025). Consequently, the impacts on water resources and agriculture may be more severe and immediate than initially anticipated.

Public health risks are also rising. Vulnerable populations—particularly the elderly, children, and those with chronic illnesses—are experiencing increased morbidity and mortality related to heat (Hayhoe et al., 2010; Arsad et al., 2022). In Amman, an average of 6.5 deaths per day have been attributed to extreme temperatures, underscoring the increased vulnerability of these populations (Alwadi et al., 2024). The rising demand for cooling days is straining Jordan's energy infrastructure, while a decrease demand in heating days offers only limited relief (MoEnv, 2022). These sectoral vulnerabilities are not isolated but are deeply interconnected. The strong correlation between WSDI and TX90p (r=0.88) suggests that prolonged heatwaves are a fundamental aspect of Jordan's climate system. This situation necessitates integrated and proactive adaptation strategies rather than isolated reactive measures.

4.3 Zonal adaptation strategies

Jordan has four Köppen climate zones: Csa, BSh, BWk, and BWh that exhibit distinct vulnerabilities and require tailored adaptation responses. Reduced frost periods threaten crops like potatoes and olives. Protected agriculture, heat-resilient varieties, and efficient water-use programs are recommended in the Csa zone (Al-Eisawi, 2005; FAO, 2023). Urban heat island effects intensify warming in the BSh zone. Rooftop gardens, tree planting, and water-conserving infrastructure can mitigate thermal stress in this zone (Shatnawi et al., 2025). Drought and rangeland degradation are key concerns in the BWk zone. Drought-tolerant crops, flexible grazing systems, and early warning mechanisms are essential (Alzboon et al., 2021). The BWh zone faces the steepest warming. Biodiversity hotspots like Dana and Azraq regions are under threat from groundwater depletion and heat stress. Desalination, conservation policies, and heatwave alerts are critical in these regions (Al-Eisawi, 2005; Ta'any et al., 2014). Comprehensive solutions such as climate-smart agriculture, precision irrigation, resilient infrastructure, and inclusive planning frameworks are necessary (Al Qudah et al., 2021; Al-Zghoul and Al-Homoud, 2025). Integrating spatial climate metrics with socio-economic vulnerability assessments will enhance predictive capacity and support targeted interventions.

4.4 Policy and research implications

The clear evidence of increasing heat extremes and ongoing climate change outlined in this study requires a shift from reactive crisis management to proactive and evidence-based climate risk governance. Policy frameworks should focus on establishing strong early warning systems and heat action plans, specifically those designed for vulnerable communities. Additionally, implementing strict groundwater protection policies to prevent over-extraction and promote climate-smart agriculture is needed to ensure food security (Ebi et al., 2021; MoEnv, 2022; UNEP, 2022). To support these policies, scientific research must progress through high-resolution regional climate modeling to decrease uncertainty in projections, which includes developing dynamic vulnerability maps that incorporate both climatic and socio-economic data, as well as conducting longitudinal studies to evaluate the effectiveness of adaptation interventions (Frame et al., 2018; Siders et al., 2019). Further climate analyses should also explore the impacts of large-scale teleconnections, such as the El Niño-Southern Oscillation (ENSO) and the Pacific

Decadal Oscillation (PDO), on extreme weather events in Jordan. These measures will enhance predictive capabilities and strengthen regional resilience strategies (Newman et al., 2016; Huang et al., 2023). By establishing a robust framework for monitoring heat extremes and linking them to sectoral vulnerabilities, this study lays the groundwork for improving evidence-based climate governance and supports Jordan's essential transition toward a more resilient and secure future.

4.5 Limitations

This study offers a detailed spatial analysis of extreme temperature trends across Jordan. However, the use of least squares regression with the RClimDex program does not consider temporal autocorrelation. Future research may investigate other non-parametric methods. The grid coverage may not accurately reflect microclimatic variations, particularly in areas with complex terrain or dense urbanization. The Köppen classification framework falls short in incorporating dynamic socioeconomic factors. Future climate change adaptation planning should integrate multi-sectoral data.

5 Conclusions

An analysis of long-term spatial trends and regime shifts in extreme temperature indices has been conducted across the diverse climate zones of Jordan. By utilizing high-resolution daily data and internationally recognized indices, the study revealed a consistent and statistically significant warming trend over the past 40 a. There has been a systematic decline in cold extremes, while heat-related events, particularly in desert zones, have intensified. A significant change point was observed around 1998, marking the onset of a heat-dominated climate regime that has continued to evolve since 2010. To identify structural climate transitions, the analysis integrated percentile-based indices, duration metrics, and correlation network structures. This methodological framework provides a spatially explicit and temporally robust assessment, offering critical insights for climate adaptation planning in arid and semi-arid environments. The vulnerabilities of various sectors, especially agriculture, water resources, and public health, are closely linked to the observed thermal shifts. The findings highlight the urgent need for heat-resilient infrastructure, precision irrigation, and early warning systems. By applying the Köppen climate classification and spatial zoning, the study highlights regional disparities in climate impacts, reinforcing the necessity for tailored adaptation strategies. Future research may investigate teleconnection influences and incorporate socio-economic data to improve vulnerability assessments.

Conflict of interest

The authors declare that they have no known competing financial interests or personal relationships that could have appeared to influence the work reported in this paper.

Acknowledgments

We thank the Al-Balqa Applied University, Jordan and the Ajloun National University, Jordan for the efforts in supporting this scientific research.

Author contributions

Conceptualization, writing - original draft preparation, and writing - review and editing: Abdelaziz Q BASHABSHEH; Supervision and writing - review and editing: Kamel K ALZBOON; Conceptualization, formal analysis, writing - review and editing, and supervision: Zeyad ALSHBOUL. All authors approved the manuscript.

References

Abu-Allaban M, Sada A, Al-Malabeh A. 2015. Temporal and spatial analysis of climate change at northern Jordanian Badia.

Carpathian Journal of Earth and Environmental Sciences, 7(2): 87–93.

Al-Bilbisi H. 2013. Topography and morphology. In: Ababsa M. Atlas of Jordan: History, Territories and Society. Beyrouth: Ifpo Press, 42–46.

Al-Eisawi D M H. 2005. Water scarcity in relation to food security and sustainable use of biodiversity in Jordan. In: Hamdy A, Monti R. Food Security under Water Scarcity in the Middle East: Problems and Solutions. Bari: CIHEAM, 239–248.

Al-Qinna M I. 2018. Analyses of climate variability in Jordan using topographic auxiliary variables by the CoKriging technique. Jordan Journal of Earth and Environmental Sciences, 9(1): 67–74.

Al Qudah A, Rusan M J, Al-Qinna M I, et al. 2021. Climate change vulnerability assessment for selected agricultural responses at Yarmouk River Basin Area, Jordan. Mitigation and Adaptation Strategies for Global Change, 26(1): 3, doi: 10.1007/s11027-021-09944-7.

Al-Zghoul S, Al-Homoud M. 2025. GIS driven spatial planning for resilient communities: Walkability, social cohesion, and green infrastructure in peri urban Jordan. Sustainability, 17(14): 6637, doi: 10.3390/su17146637.

Ali S, Saeed A, Kiani R S, et al. 2021. Future climatic changes, extreme events, related uncertainties, and policy recommendations in the Hindu Kush sub-regions of Pakistan. Theoretical and Applied Climatology, 143(1): 193–209.

Alsalal S, Tan M L, Samat N, et al. 2024. Temperature and precipitation changes under CMIP6 projections in the Mujib Basin, Jordan. Theoretical and Applied Climatology, 155(8): 7703–7720.

Alwadi Y, Al-Delaimy W K, Abdulla F, et al. 2024. A 19-year analysis of hot and cold temperature burdens on mortality in Amman, Jordan. Science of the Total Environment, 951: 175624, doi: 10.1016/j.scitotenv.2024.175624.

Alzboon K, Al-Samrraie L A, Al Bkoor Alrawashdeh K. 2021. Climate change indicators in Jordan: A new approach using area method. Jordan Journal of Civil Engineering, 15(1): 142–155.

Armstrong McKay D I, Staal A, Abrams J F, et al. 2022. Exceeding 1.5°C global warming could trigger multiple climate tipping points. Science, 377(6611): eabn7950, doi: 10.1126/science.abn7950.

Arsad F S, Hod R, Ahmad N, et al. 2022. The impact of heatwaves on mortality and morbidity and the associated vulnerability factors: A systematic review. International Journal of Environmental Research and Public Health, 19(23): 16356, doi: 10.3390/ijerph192316356.

Atashi N, Rahimi D, Al Kuisi M, et al. 2020. Modeling long term temporal variation of dew formation in Jordan and its link to climate change. Water, 12(8): 2186, doi: 10.3390/w12082186.

Baig M A, Zaman Q, Baig S A, et al. 2021. Regression analysis of hydro-meteorological variables for climate change prediction: a case study of Chitral Basin, Hindukush region. Science of the Total Environment, 793: 148595, doi: 10.1016/j.scitotenv.2021.148595.

Bashabsheh A Q, Alzboon K K. 2024. Impact of climate change on water resources in the Yarmouk River Basin of Jordan. Journal of Arid Land, 16(12): 1633–1647.

Bashabsheh A Q, Alzboon K K. 2025. Climate change in Jordan: a case study of Yarmouk Basin using statistical downscaling model. Jordan Journal of Civil Engineering, 19(4): 503–527.

Bisht H, Shaloo B, Kumar B, et al. 2023. Sensitivity analysis of wheat cultivar HD2967 to weather parameters using CERES-Wheat model. Journal of Agricultural Science and Technology, 25(3): 661–672.

Cartwright S L, Schmied J, Karrow N, et al. 2023. Impact of heat stress on dairy cattle and selection strategies for thermotolerance: a review. Frontiers in Veterinary Science, 10: 1198697, doi: 10.3389/fvets.2023.1198697.

Cheng Q P, Zhong F L, Wang P. 2021. Potential linkages of extreme climate events with vegetation and large-scale circulation indices in an endorheic river basin in northwest China. Atmospheric Research, 247: 105256, doi: 10.1016/j.atmosres.2020.105256.

Cheong W K, Timbal B, Golding N, et al. 2018. Observed and modelled temperature and precipitation extremes over Southeast Asia from 1972 to 2010. International Journal of Climatology, 38(7): 3013–3027.

Douris J, Kim G. 2021. Atlas of Mortality and Economic Losses from Weather, Climate and Water Extremes (1970–2019). Geneva: World Meteorological Organization.

Easterling D R, Alexander L V, Mokssit A, et al. 2003. CCl/CLIVAR workshop to develop priority climate indices. American Meteorological Society. [2025-04-06]. https://etccdi.pacificclimate.org/papers/EasterlingetalOct03BAMS.pdf.

Ebi K L, Capon A, Berry P, et al. 2021. Hot weather and heat extremes: health risks. The Lancet, 398(10301): 698–708.

Eckstein D, Künzel V, Schäfer L. 2021. Global Climate Risk Index 2021. Bonn: Germanwatch.

FAO (Food and Agriculture Organization of the United Nations). 2023. Jordan Climate Smart Agriculture Action Plan: Investment Opportunities in the Agriculture Sector's Transition to a Climate Resilient Growth Path. Rome: Food and Agriculture Organization of the United Nations.

Frame B, Lawrence J, Ausseil A-G, et al. 2018. Adapting global shared socio-economic pathways for national and local scenarios. Climate Risk Management, 21: 39–51.

Guijarro J A. 2018. Homogenization of climatic series with Climatol. [2025-02-08]. https://repositorio.aemet.es/bitstream/20.500.11765/12185/2/homog_climatol.-en.pdf

Hamdi M, Abu-Allaban M, Al-Shayeb A, et al. 2009. Climate change in Jordan: a comprehensive examination approach. American Journal of Environmental Sciences, 5(1): 58–68.

Hayhoe K, VanDorn J, Croley T, et al. 2010. Regional climate change projections for Chicago and the US Great Lakes. Journal of Great Lakes Research, 36(S2): 7–21.

Hazaymeh K, Zeitoun M, Almagbile A, et al. 2024. Exploring the dynamics of land surface temperature in Jordan's local climate zones: a comprehensive assessment through Landsat entire archive and Google Earth Engine. Atmosphere, 15(3): 318, doi: 10.3390/atmos15030318.

Hoag H. 2014. Russian summer tops 'universal' heatwave index. Nature, 510(7504): 16250, doi: 10.1038/nature.2014.16250.

Huang C M, Liu H L, Li H, et al. 2023. Combined effects of ENSO and PDO on activity of major hurricanes in the Eastern North Pacific. Climate Dynamics, 2: 1467–1486.

Hussain A, Cao J H, Ali S, et al. 2022. Wavelet coherence of monsoon and large-scale climate variabilities with precipitation in Pakistan. International Journal of Climatology, 42(16): 9950–9966.

IPCC (Intergovernmental Panel on Climate Change). 2019. Climate Change and Land: An IPCC Special Report on Climate Change, Desertification, Land Degradation, Sustainable Land Management, Food Security, and Greenhouse Gas Fluxes in Terrestrial Ecosystems. Geneva: IPCC.

IPCC (Intergovernmental Panel on Climate Change). 2022. Impacts, Adaptation, and Vulnerability. Contribution of Working Group II to the Sixth Assessment Report of the Intergovernmental Panel on Climate Change. Geneva: IPCC.

IPCC (Intergovernmental Panel on Climate Change). 2023. Climate change 2023: Synthesis report. Contribution of Working Groups I, II and III to the Sixth Assessment Report of the Intergovernmental Panel on Climate Change. Geneva: IPCC.

Köppen W, Wegener A. 2015. The Climates of the Geological Past. Stuttgart: Borntraeger Scientific Publishers.

Linnenluecke M K, Griffiths A, Winn M I. 2013. Firm and industry adaptation to climate change: a review of climate adaptation studies in the business and management field. WIREs Climate Change, 4(5): 397–416.

Marzouk O A. 2021. Assessment of global warming in Al Buraimi, Sultanate of Oman, based on statistical analysis of NASA POWER data over 39 years, and testing the reliability of NASA POWER against meteorological measurements. Heliyon, 7(3): e06625, doi: 10.1016/j.heliyon.2021.e06625.

MoEnv (Ministry of Environment). 2022. National adaptation plan (NAP): The Hashemite Kingdom of Jordan. Amman: MoEnv. [2025-04-15]. https://www.moenv.gov.jo/ebv4.0/root_storage/en/eb_list_page/national_adaptation_plan.pdf.

Newman M, Alexander M A, Ault T R, et al. 2016. The Pacific Decadal Oscillation, revisited. Journal of Climate, 29(12): 4399–4427.

Pascal M, Wagner V, Lagarrigue R, et al. 2024. A yearly measure of heat-related deaths in France, 2014–2023. Discover Public Health, 21(1): 44, doi: 10.1186/s12982-024-00164-3.

Perera A T D, Nik V M, Chen D L, et al. 2020. Quantifying the impacts of climate change and extreme climate events on energy systems. Nature Energy, 5(2): 150–159.

Resource Watch. 2025. Water stress country ranking. Washington DC: World Resources Institute. [2025-06-30]. https://resourcewatch.org/data/explore/wat036rw1-Water-Stress-Country-Ranking.

Rodrigues G C, Braga R P. 2021. Evaluation of NASA POWER reanalysis products to estimate daily weather variables in a hot summer Mediterranean climate. Agronomy, 11(6): 1207, doi: 10.3390/agronomy11061207.

Safriel U. 2017. Land degradation neutrality (LDN) in drylands and beyond–where has it come from and where does it go? Silva Fennica, 51(1):1650, doi: 10.14214/sf.1650.

Shatnawi N, Alqaralleh R M, Tarawneh E R. 2025. Urban heat island in Amman: AI-based modeling of urban morphology and green infrastructure in mitigating thermal stress. Environmental Earth Sciences, 84(17): 498, doi: 10.1007/s12665-025-12507-7.

Siders A R, Hino M, Mach K J. 2019. The case for strategic and managed climate retreat. Science, 365(6455): 761–763.

Smadi M M. 2006. Observed abrupt changes in minimum and maximum temperatures in Jordan in the 20th century. American Journal of Environmental Sciences, 2(3): 114–120.

Ta'any R, Masalha L, Khresat S E, et al. 2014. Climate change adaptation: a case study in Azraq Basin, Jordan. International Journal of Current Microbiology and Applied Sciences, 3: 108–122.

UNEP (United Nations Environment Programme). 2022. Adaptation gap report 2022: Too little, too slow–climate adaptation

failure puts world at risk. Nairobi: UNEP. [2025-04-15]. https://www.unep.org/resources/adaptation-gap-report-2022.

WMO (World Meteorological Organization). 2024. WMO confirms that 2023 smashes global temperature record. Geneva: WMO. [2025-04-16]. https://wmo.int/news/media-centre/wmo-confirms-2023-smashes-global-temperature-record.

World Bank Group. 2025. The World Bank in Jordan. Washington DC: World Bank Group. [2025-04-30]. https://climateknowledgeportal.worldbank.org/country/jordan.

Zeppel M, Lewis J, Phillips N, et al. 2014. Consequences of nocturnal water loss: A synthesis of regulating factors and implications for capacitance, embolism and use in models. Tree Physiology, 34(10): 1047–1055.

Zhang X, Yang F. 2004. RClimDex (1.0)—User manual. Climate Research Branch, Environment Canada, Downsview, Ontario. [2025-04-30]. https://studylib.net/doc/7659063/rclimdex-1-climate-change-indices.

Zhang X B, Alexander L, Hegerl G C, et al. 2011. Indices for monitoring changes in extremes based on daily temperature and precipitation data. WIREs Climate Change, 2(6): 851–870.

Zhu H F, Shao X M, Zhang H, et al. 2019. Trees record changes of the temperate glaciers on the Tibetan Plateau: Potential and uncertainty. Global and Planetary Change, 173: 15–23.

Zittis G, Almazroui M, Alpert P, et al. 2022. Climate change and weather extremes in the Eastern Mediterranean and Middle East. Reviews of Geophysics, 60(3): e2021RG000762, doi: 10.1029/2021RG000762.